Cascade system using both trough system and dish system for power generation

1 Introduction

Energy is the crucial part for the infrastructure and maintenance of society. With the increase amount of energy consumption, our quality of life has been improved significantly. However, nowadays the world energy consumption is highly dependent on fossil fuels, which supplied 81.3% of the world's energy consumption in 2012 according to the data of World Bank Group. Using fossil fuels a lot is afflicting the environment, which is sacrificing our quality of life. Environmental pollutions and global warming are becoming serious problem, and it is urgent to find clean and renewable energy to substitute the fossil fuels.

Solar energy is a clean, sustainable, wide-distributed energy. The total amount of solar energy is very huge. The amount of sunlight striking the earth's atmosphere continuously is 1.75×10^5 TW, even if 1% of it could be converted into electric energy with a 10% efficiency, it would produce 175 TW, much larger than the total global energy needs predicted to be 25?30 TW in 2050 [1]. But at the same time, solar energy has some disadvantages for its low flux density and large fluctuation due to daily and seasonal variations exacerbated by variations owing to weather. Concentrated solar power (CSP) technology has the ability to overcome these disadvantages and believed to be the future power generation technology.

There are 4 common forms of CSP technologies, parabolic trough, dish Stirlings, concentrating linear Fresnel receiver, and solar power tower. Different types of collectors and different technologies for electricity generation are suitable for different working temperature zones with different costs. Combination of different collectors with different technologies may provide a new direction to achieve higher efficiency with lower cost for CSP.

Cau [2] reported a comparative performance analysis of CSP plants using parabolic trough and linear Fresnel collectors, thermal oil as heat transfer fluid and an Organic Rankine Cycle (ORC) power generation unit. A two-tank direct thermal storage system are included and in the Rankine cycle, regenerator, 4 6 steam extractions and air-cooler condenser are used. The performance analysis of the two types of system shows that CSP plants based on linear Fresnel collectors lead to higher values of electrical energy production per unit area of land and CSP plants based on parabolic troughs gives better values of energy production per unit area of collector.

Franchini [3] carried out simulations to predict the performance of a Solar Rankine Cycle (SRC) and an Integrated Solar Combined Cycle (ISCC) when combined with two different solar field configurations based on parabolic trough collectors (PTCs) and power tower (PT) systems. The comparative analysis was mainly focused on the influence of CSP technology on global solar energy conversion efficiency of both SRC and ISCC plants. Results show that both higher collection efficiency and conversion efficiency of ST compared to PTCs in both SRC and ISCC situations.

Cipollone [4] discussed some thermodynamic and engineering aspects concerning the use of parabolic troughs for heating gasses of gas turbines. They further discussed the Discrete Ericsson Cycle (DEC), in the cycle, a sequence of intercooled compressions and reheated expansions is deployed to increase cycle specific work and efficiency. They applied optimization adopting as design parameter the power per unit of collector length, and pointed out that the number of

compressions and expansions could not exceed three stages.

Behar [5] reviewed the R&D activities and published studies on integrated solar combined cycle system (ISCCS), various configurations have been proposed with their performance investigated. The paper also introduced lots of software or mathematical programs to simulate the performance of various design.

Ghaem [6] investigated and compared the performance of various configurations of hybrid solar dish-Brayton cycle. A thermodynamic model implemented in Engineering Equation Solver (EES) is developed for various configurations. Results show that the model in which receiver located before the turbine can achieve higher performance compare to the one in which the receiver located after the turbine. Simulation of the models pointed out that a comprehensive well defined control algorithm is a vital issue in order to control engine operation, solar input heat flux and sun tracking system.

In this paper, an idea of cascade collection and cascade utilisation of solar energy with higher efficiency is presented. Parabolic trough collectors are used to collect lower temperature energy with lower cost and dish collectors are used to collect higher temperature energy with higher efficiency. Rankine cycle is used to work in lower temperature zone and Stirling cycle is used to work in higher temperature zone. Furthermore, effective topological structures are considered to take full advantages of thermodynamic characters of different components of the system. The cold chamber of Stirling engine is cooled by condensed fluid of Rankine cycle to use the heat released by Stirling engine.

First, the idea of cascade system is presented and the feasibility analysis of the system is performed. A conceptual sketch of the system is presented with some important state points. Second, based on this sketch, some components are chosen and some key parameters of the system are given. Third, models of components are built according to their thermodynamic properties. Models of different circuits are built with these component models and efficiency can be obtained by the circuit data. Fourth, two separate systems, dish-Stirling system and trough-Rankine system, are built for comparison. At last, the models of the systems are calculated and results are analysed.

2 System description and specification

In the cascade system, dish collectors are used to provide heat for Stirling engines and air-to-water heat exchanger. Trough collectors are used to provide heat for preheating, evaporating and superheating in the Rankine cycle. Figure 1 shows the sketch of the cascade system. Water is used as the working fluid of Rankine cycle, which is heated in the cold chamber of Stirling engines, preheater, evaporator, superheater, and air-to-water heat exchanger successively, and then expand in turbine, condense in condenser. Pumps are used to change the pressure of fluids. Stirling engines are used for power generation and cooled by feed water of the Rankine cycle. State number pairs of different fluids are marked on the sketch. The first number of a number pair indicates the type of the fluid, the second number of a number pair indicates the state point of the fluid. Number pairs with solid circle indicate saturated liquid states ($x = 0$), and with dotted circle indicates saturated gas states ($x = 1$). Figure 2 shows the T-s diagram of the water circuit in the cascade system. In this Rankine cycle, the heat released in "2,5-2,6" process can be utilized by series of Stirling engines, which may increase the power of Rankine cycle. Figure 3 shows the heat transfer diagram of this process.

To build the cascade system model, several simplifying assumptions are made:

- Steady state at nominal load of the system is analyzed
- Pressure drop due to flow is negligible
- The leak of working fluid in the pipes is neglected

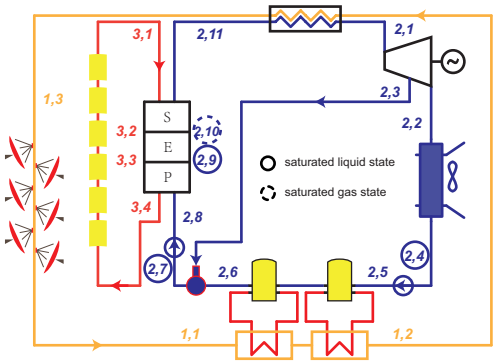

Figure 1: Sketch of the cascade system

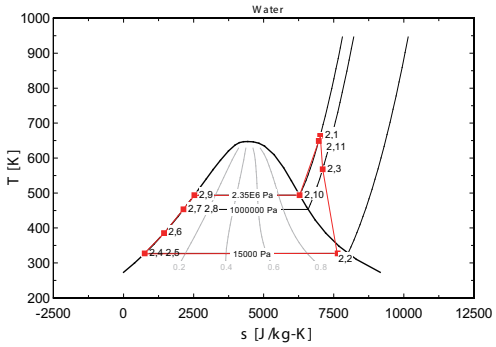

Figure 2: T-s diagram of the water circuit

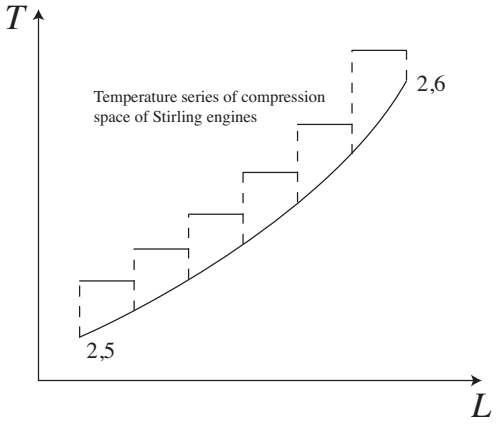

Figure 3: Heat transfer diagram of "2,5-2,6" process

- Same isentropic efficiency of steam turbine with different loads and in different stages
- Heat loss that occurs from the tube to the atmosphere is not considered
- There is no heat loss to the environment for Stirling engines
- Simple models are used of some processes and equipments
- A symmetrical regenerator behaviour is assumed so that a single effectiveness can be defined as $e = \frac{T_R - T_L}{T_H - T_L}$ [7, 8]

Table 1 shows the basic design parameters of the cascade system.

3 System model

An EES model was built to investigate the characteristics of the cascade system. The cascade system is built in several blocks. These blocks are made of circuits with efficiency calculations. Three circuits, air circuit, water circuit and oil circuit, are built with some specific state parameters in some key components. Energy-based models of these key components are created on the basis of their thermodynamic behavior, heat transfer and the second law.

The following parts introduce models of some key components.

3.1 Dish receiver

Fraser, in his dissertation [9], built a performance prediction model of Stirling dish system with detailed description. The model is also used in the software SAM, which provides performance and financial models for facilitate decision in the renewable energy industry. The dish collector model in the dissertation considers various heat losses, which is a good reference for the dish receiver model of the cascade system.

Table 1: Basic design parameters of the cascade system

Parameters	Value
I_{DNI}	700 W/m^2
T_{amb}	293 K
p_{amb}	1×10^5 Pa
v_{wind}	4 m/s
$P_{generator}$	6×10^6 W
$T_{dish,inlet}$	623K
$T_{dish,outlet}$	1073 K
p_{dish}	5×10^5 Pa
$A_{dishCollector}$	87.7 m^2
$\Delta T_{oil,water,min}$	15 K
$T_{trough,outlet}$	623 K
p_{trough}	2×10^6 Pa
$A_{troughCollector}$	545 m^2
$T_{1,afterstirling}$	673 K
n_{se}	10 s^{-1}
$U_{stirling,1}$	30 W/(m^2·K)
$U_{stirling,2}$	150 W/(m^2·K)
$A_{stirling,1}$	8 m^2
$A_{stirling,2}$	8 m^2
$k_{stirling}$	1.4
$\gamma_{stirling}$	3.375
n	7.73×10^{-2} mol
$n_{stirlingEngine}$	100
T_s	340°C
p_s	2.35×10^6 Pa
p_c	1.5×10^4 Pa
$T_{s,d}$	390°C
$p_{c,p}$	1×10^6 Pa
$p_{deaerator}$	1×10^6 Pa

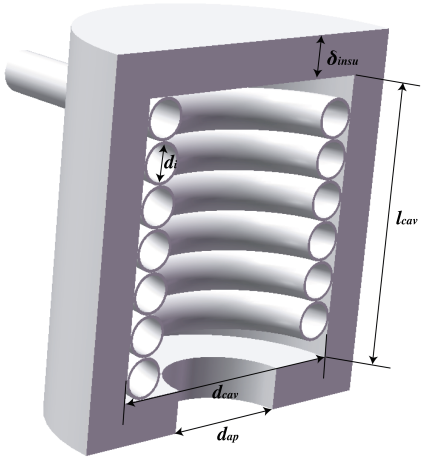

Figure 4: Structure of the dish receiver

In our cascade system, the structure of the dish receiver is as shown in Figure 4. The dish receiver model concerns the losses includes: collector losses due to mirror reflectivity, receiver intercept losses, losses due to shading, and thermal losses. Thermal losses take the largest portion of all those losses, which are due to conduction, convection and radiation. Figure 5 shows the heat network of dish receiver, which concerns the losses:

- Radiation losses reflected off of the receiver cavity surfaces and out of the receiver through the aperture. ($q_{rad,reflect}$)
- Conductive losses through the receiver insulating layer. ($q_{cond,tot}$)
- Free convection from the cavity in the absence of wind. ($q_{conv,free}$)
- Forced convection in the presence of wind. ($q_{conv,forced}$)
- Emission losses due to thermal radiation emitted from the receiver aperture. ($q_{rad,emit}$)

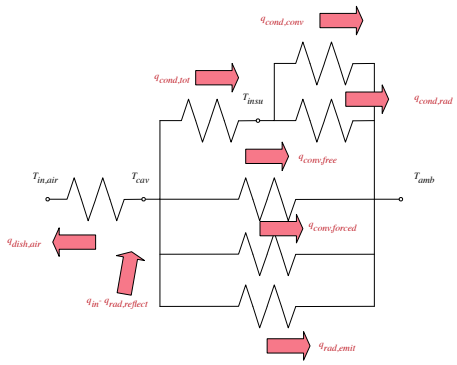

Figure 5: Heat network of dish receiver

A dish collector product of SES used in Fraser's paper, which is also used in this system, and its parameters are listed in Table 2 [9].

Table 2: Parameters of the dish receiver

Parameters	Value
d_{cav}	0.46 m
δ_{insu}	0.075 m
l_{cav}	0.23 m
d_{ap}	0.184 m
λ_{insu}	0.06 W/(m·K)
ϵ_{insu}	0.6
α_{cav}	0.87
δ_a	0.005 m
d_i	0.07 m
θ_{dish}	45°
γ	0.97
$\eta_{shading}$	0.95
ρ	0.91

$q_{dish,air}$ can be written as

$$q_{dish,air} = h_{dish,air} A_{dish,air} \Delta T_{ln,Drec,air}$$

where

$$h_{dish,air} = Nu_{tube} \lambda_{dish,air} / d_i$$

$$Nu_{tube} = c_r Nu_{tube}^{'}$$

For helical spiral pipe, multiplier c_r based on curvature ratio can be written as [10]

$$c_r = 1 + 3.5 \frac{d_i}{d_{cav} - d_i - 2\delta_a}$$

$Nu_{tube}^{'}$ is the Nusselt number of straight circular tube, which can be obtained by [11]

$$Nu_{tube}^{'} = 0.027 Re_{tube}^{0.8} Pr_{tube}^{1/3} (\mu_{tube}/\mu_{tube,w})^{0.14}$$

$$c_r = 1 + 3.5 \frac{d_i}{d_{cav} - d_i - 2\delta_a}$$

and $\Delta T_{ln,Drec,air}$ can be written as

$$\Delta T_{ln,Drec,air} = \frac{(T_{cav} - T_{dish,inlet}) - (T_{cav} - T_{dish,outlet})}{\ln \frac{T_{cav} - T_{dish,inlet}}{T_{cav} - T_{dish,outlet}}}$$

To get $q_{dish,air}$, T_{cav} is required. As shown in Figure 5, we need to solve the heat network.

$$q_{in} = q_{rad,reflect} + q_{dish,air} + q_{cond,tot} + q_{conv,tot} + q_{rad,emit} \quad (1)$$

q_{in} can be obtained by

$$q_{in} = I_{DNI} \cdot A_{dishCollector} \gamma \eta_{shading} \rho \quad (2)$$

Other losses are presented in following sections.

3.1.1 Reflected loss of dish receiver

To determine the reflected loss of the cavity surfaces of the dish receiver $q_{rad,reflect}$, the effective absorptance of the cavity receiver α_{eff} is required to determine the fraction of energy reflected out of the receiver. The effective absorptance of a cavity receiver without a receiver aperture cover is given by Equation (3) where α_{cav} is the cavity surface absrptance, A_a is the cavity aperture area, and A_{cav} is the

total inner surface area of the cavity [12]. Sandra National Laboratories gave an estimate value of the absorptance of the cavity surface α_{cav} of an existing Stirling dish receiver to be 0.87 [13]. To achieve higher effective absorptance, a smaller ratio of the two surface area should be used. But the ratio is constrained by the concentration ratio of the receiver.

$$\alpha_{eff} = \frac{\alpha_{cav}}{\alpha_{cav} + (1 - \alpha_{cav})\,(A_{ap}/A_{cav})} \tag{3}$$

$$q_{rad,reflect} = q_{in}(1 - \alpha_{eff})$$

3.1.2 Conduction loss of dish receiver

Conduction loss of dish receiver $q_{cond,tot}$ equals to the different two parts: convection loss from the insulating layer to the atmosphere $q_{cond,conv}$ and radiation loss from the insulating layer to the atmosphere $q_{cond,rad}$. Both of the two parts are related to the temperature of insulating layer T_{ins}.

$$q_{cond,tot} = \frac{T_{cav} - T_{insu}}{\ln\dfrac{d_{cav} + 2\delta_{insu}}{d_{cav}}/(2\pi\lambda_{insu}l_{cav})}$$

$$\begin{aligned} q_{cond,conv} &= h_{insu}A_{insu}(T_{insu} - T_{amb}) \\ &= \frac{k_{insu}Nu_{insu}A_{insu}(T_{insu} - T_{amb})}{d_{cav} + 2\delta_{insu}} \end{aligned}$$

$$q_{cond,rad} = \epsilon_{insu}A_{insu}\sigma(T_{insu}^4 - T_{amb}^4)$$

And

$$q_{cond,tot} = q_{cond,conv} + q_{cond,rad}$$

3.1.3 Convection loss of dish receiver

Ma [14] conducted tests to determine the free convection losses from the receiver for alternative setups, and the data were consistent with Stine and McDonald's free convection correlation. It is assumed that forced convection is independent of free convection in the receiver, so the total convection losses can be represented as the sum of the free and forced convection losses as shown in Figure 5.

$$q_{con,tot} = q_{con,free} + q_{con,forced}$$

3.2 Stirling engine array

The layout of the Stirling engine array is shown in Figure 6. n_1 is chosen to be 10 and can be optimized later.

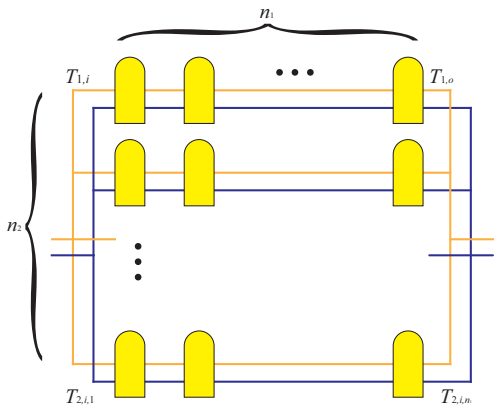

Figure 6: Layout of Stirling engines

$$T_{1,i,1} = T_{1,i}$$

$$q_{m,1,r} = q_{m,1}/n_2$$

where $n_2 = n_{stirlingEngine}/n_1$.

If the flow type between the heating and cooling flows is parallel flow,

$$T_{2,i,1} = T_{2,i}$$

$$q_{m,2,r} = q_{m,2}/n_2$$

If the flow type between the heating and cooling flows is counter flow,

$$T_{2,o,n_1} = T_{2,i}$$

$$q_{m,2,r} = -q_{m,2}/n_2$$

For a Stirling engine in column x, x from 1 to n_1, $c_{p,1,x}$ and $c_{p,2,x}$ can be written as

$$c_{p,1,x} = g_1(T_{1,i,x}, T_{1,o,x})$$

$$c_{p,2,x} = g_2(T_{2,i,x}, T_{2,o,x})$$

According to Appendi,

$$T_{H,x} = T_{1,i,x} - \frac{T_{1,i,x} - T_{1,o,x}}{1 - \exp(-\frac{U_{stirling,1}A_{stirling,1}}{q_{m,1,r}c_{p,1,x}})}$$

$$T_{L,x} = T_{2,i,x} - \frac{T_{2,i,x} - T_{2,o,x}}{1 - \exp(-\frac{U_{stirling,2}A_{stirling,2}}{q_{m,2,r}c_{p,2,x}})}$$

Because of Equation (3.2) and (3.2), Equation (3.2) and (3.2) can be written as

$$T_{H,x} = g_3(T_{1,i,x}, T_{1,o,x})$$

$$T_{L,x} = g_4(T_{2,i,x}, T_{2,o,x})$$

Choose $T_{R,x} = \frac{T_{H,x} - T_{L,x}}{\ln(T_{H,x}/T_{L,x})}$, and $e_x = \frac{T_{R,x} - T_{L,x}}{T_{H,x} - T_{L,x}}$, then

$$\eta_{stirling,x} = \frac{T_{H,x} - T_{L,x}}{T_{H,x} + \frac{1 - e_x}{k - 1} \cdot \frac{T_{H,x} - T_{L,x}}{\ln \gamma_{stirling}}}$$

which can be written as

$$\eta_{stirling,x} = g_5(T_{1,i,x}, T_{1,o,x}, T_{2,i,x}, T_{2,o,x})$$

On the other way, for x from 1 to n_1,

$$h_{1,i,x} = h_1(T_{1,i,x})$$

$$h_{1,o,x} = h_1(T_{1,o,x})$$

$$h_{2,i,x} = h_2(T_{2,i,x})$$

$$h_{2,o,x} = h_2(T_{2,o,x})$$

For energy balance,

$$q_{m,1,r}(h_{1,i,x} - h_{1,o,x})(1 - \eta_{stirling,x}) = q_{m,2,r}(h_{2,o,x} - h_{2,i,x})$$

which can be written as

$$h_3(\eta_{stirling,x}, T_{1,i,x}, T_{1,o,x}, T_{2,i,x}, T_{2,o,x}) = 0$$

for $q_{m,1,r}$ and $q_{m,2,r}$ can be obtained once the flow type is known.

And in Stirling cycle, the heat absorbed by the working gas is

$$nR\left(T_{H,x}\ln\gamma_{stirling} + \frac{1 - e_x}{k - 1}(T_{H,x} - T_{L,x})\right) = q_{m,1,r}(h_{1,i,x} - h_{1,o,x})/$$

can be written as

$$f(T_{1,i,x}, T_{1,o,x}) = 0$$

And for x from 1 to $n_1 - 1$,

$$T_{1,i,x+1} = T_{1,o,x}$$

$$T_{2,i,x+1} = T_{2,o,x}$$

Solve the simultaneous equations for x from 1 to n_1: Equation (3.2), (3.2) (or (3.2)), (3.2), (3.2), (3.2), (3.2) ($5n_1$ equations with $5n_1$ variables), we can get $T_{2,i,1}, T_{2,o,n_1}$ and then use $h_{2,i,1}, h_{2,o,n_1}$ to get $\eta_{stirling}$ by Equation (3.2)

$$\eta_{stirling} = 1 - \frac{q_{m,2}(h_{2,o,n_1} - h_{2,i,1})}{q_{m,1}(h_{1,i,1} - h_{1,o,n_1})}$$

and power of Stirling engine in column x

$$P_{stirlingEngine,x} = q_{m,1,r}(h_{1,i,x} - h_{1,o,x})\eta_{stirling,x}$$

and $P_{stirling}$ can be obtained by

$$P_{stirling} = \eta_{stirling}q_{m,1}(h_{1,i,1} - h_{1,o,n_1})$$

3.3 Water circuit

$\eta_{i,turbine}$ is obtained by given design parameters of the turbine.

For state $[2,1]$,

$$\left.\begin{array}{l} p_{2,1} = p_s \\ T_{2,1} = T_s \end{array}\right\} \Rightarrow \left\{\begin{array}{l} h_{2,1} \\ s_{2,1} \end{array}\right.$$

For state $[2,2]$,

$$\left.\begin{array}{l} s_{i,2,2} = s_{2,1} \\ p_{i,2,2} = p_c \end{array}\right\} \Rightarrow h_{i,2,2}$$

$$\eta_{i,turbine} = \frac{h_{2,1} - h_{2,2}}{h_{2,1} - h_{i,2,2}}$$

$$\left.\begin{array}{l} p_{2,2} = p_c \\ h_{2,2} \end{array}\right\} \Rightarrow \left\{\begin{array}{l} T_{2,2} \\ x_{2,2} \end{array}\right.$$

For state $[2,3]$

$$\left.\begin{array}{l} s_{i,2,3} = s_{2,1} \\ p_{i,2,3} = p_{deaerator} \end{array}\right\} \Rightarrow h_{i,2,3}$$

$$\eta_{i,turbine} = \frac{h_{2,1} - h_{2,3}}{h_{2,1} - h_{i,2,3}}$$

$$\left.\begin{array}{l} p_{2,3} = p_{deaerator} \\ h_{2,3} \end{array}\right\} \Rightarrow \left\{\begin{array}{l} T_{2,3} \\ x_{2,3} \end{array}\right.$$

$$P_{turbine} = P_{generator}/\eta_{generator}$$

$$P_{turbine} = (1-y)\, q_{m,2}\, (h_{2,1} - h_{2,2}) + y q_{m,2}\, (h_{2,1} - h_{2,3})$$

For state $[2,4]$,

$$\left.\begin{array}{l} p_{2,4} = p_{2,2} \\ x_{2,4} = 0 \end{array}\right\} \Rightarrow \left\{\begin{array}{l} h_{2,4} \\ s_{2,4} \end{array}\right.$$

For state $[2,5]$,

$$\left.\begin{array}{l} p_{2,5} = p_{2,stirling} \\ s_{2,5} = s_{2,4} \end{array}\right\} \Rightarrow \left\{\begin{array}{l} T_{2,5} \\ h_{2,5} \end{array}\right.$$

For state $[2,6]$,

$$q_{stirling,cold} = (1-y)\, q_{m,2}\, (h_{2,6} - h_{2,5}) \Rightarrow h_{2,6}$$

$$\left.\begin{array}{l} p_{2,6} = p_{2,5} \\ h_{2,6} \end{array}\right\} \Rightarrow \left\{\begin{array}{l} T_{2,6} \\ s_{2,6} \end{array}\right.$$

For state $[2,7]$,

$$\left.\begin{array}{l} p_{2,7} = p_{deaerator} \\ x_{2,7} = 0 \end{array}\right\} \Rightarrow \left\{\begin{array}{l} h_{2,7} \\ s_{2,7} \end{array}\right.$$

$$y h_{2,3} + (1-y)\, h_{2,6} = h_{2,7}$$

For state $[2,8]$,

$$\left.\begin{array}{l} p_{2,8} = p_s \\ s_{2,8} = s_{2,7} \end{array}\right\} \Rightarrow \left\{\begin{array}{l} T_{2,8} \\ h_{2,8} \end{array}\right.$$

For Rankine cycle,

$$\eta_{rankine} = \frac{(1-y)\, (h_{2,1} + h_{2,4} - h_{2,2} - h_{2,5}) + y\, (h_{2,1} - h_{2,3}) - (h_{2,8} -}{(1-y)\, (h_{2,6} - h_{2,5}) + h_{2,1} - h_{2,8}}$$

For state $[2,9]$,

$$\left.\begin{array}{l} p_{2,9} = p_{2,8} \\ x_{2,9} = 0 \end{array}\right\} \Rightarrow \left\{\begin{array}{l} T_{2,9} \\ h_{2,9} \end{array}\right.$$

For state $[2,10]$,

$$\left.\begin{array}{l} p_{2,10} = p_{2,9} \\ x_{2,10} = 1 \end{array}\right\} \Rightarrow \left\{\begin{array}{l} T_{2,10} \\ h_{2,10} \end{array}\right.$$

For state $[2,11]$,

$$\left.\begin{array}{l} p_{2,11} = p_{2,10} \\ q_{m,1}\, (h_{1,2} - h_{1,3}) = q_{m,2}\, (h_{2,1} - h_{2,11}) \end{array}\right\} \Rightarrow T_{2,11}$$

$$q_{trough} = q_{m,2}\, (h_{2,11} - h_{2,8})$$

$$q_{trough} = I_p \cdot A_{trough} \cdot \eta_{trough}$$

$$n_{troughCollector} = ceil(A_{trough}/A_{troughCollector})$$

where $ceil(x)$ is a function that returns the smallest integer larger than x.

Nomenclature

$A_{dishCollector}$	Aperture area of each dish collector, m^2
$A_{stirling,1}$	Heat transfer area of Stirling engine at air side, m^2
$A_{stirling,2}$	Heat transfer area of Stirling engine at water side, m^2
$A_{troughCollector}$	Aperture area of each trough collector, m^2
A_{trough}	Aperture area of all trough collectors, m^2
d_{ap}	Aperture diameter of volumetric receiver, m
d_{cav}	Diameter of volumetric receiver cavity, m
d_i	Inner diameter of air tube, m
I_{DNI}	Direct Normal Irradiance, W/m^2
$k_{stirling}$	Specific heat ratio of the working gas in Stirling engine
l_{cav}	Depth of volumetric receiver cavity, m
n	Amount of working gas in each Stirling engine, mol
n_1	Number of columns of the Stirling engine array
n_2	Number of rows of the Stirling engine array
n_{se}	Speed of Stirling engine, s^{-1}
$n_{stirlingEngine}$	Number of Stirling engines in the Stirling engine array
$n_{troughCollector}$	Number of all trough collectors
p_c	Exhaust pressure of turbine, Pa
p_s	Main steam pressure of turbine, Pa
p_{amb}	Ambient pressure, Pa
p_{cp}	Water pressure after condensate pump, Pa
$p_{deaerator}$	Outlet pressure of deaerator, Pa
p_{dish}	Air pressure in dish, Pa
$P_{generator}$	Power of generator, W
p_{trough}	Air pressure in trough, Pa
$q_{cond,tot}$	Total conduction loss
$q_{conv,tot}$	Total convection loss
$q_{dish,air}$	Energy absorbed by air in the dish collector
q_{in}	Solar energy launched into dish receiver aperture, W
$q_{m,1,r}$	Mass flow rate of air in each row of Stirling engine array, kg/s
$q_{m,2,r}$	Mass flow rate of water in each row of Stirling engine array, kg/s
$q_{m,2}$	Total mass flow rate of water, kg/s
$q_{rad,emit}$	Radiation emitted by dish receiver
$q_{rad,reflect}$	Reflected radiation by volumetric receiver, W
T_s	Main steam temperature of turbine
$T_{1,afterstirling}$	Air temperature after heating Stirling engine

T_{amb}	Ambient temperature, K
$T_{dish,inlet}$	Dish inlet temperature, K
$T_{dish,outlet}$	Dish outlet temperature
$T_{s,d}$	Designed mean steam temperature of turbine
$T_{trough,outlet}$	Trough outlet temperature
$U_{stirling,1}$	Overall heat transfer coefficient of Stirling engine at air side, W/(m^2·K)
$U_{stirling,2}$	Overall heat transfer coefficient of Stirling engine at water side, W/(m^2·K)
v_{wind}	Ambient wind speed, m/s
x	Dryness fraction
y	Extraction rate of steam turbine

Abbreviations

EES	Engineering Equation Solver
SAM	System Advisor Model
SES	Stirling Energy System

Greek Symbols

α_{eff}	Effective absorptance
δ_a	Thickness of air tube in volumetric receiver, m
δ_{ins}	Thickness of receiver insulating layer, m
$\Delta T_{oil,water,min}$	Minimum temperature difference between oil and water in the oil-to-water heat exchanger, K
ϵ_{insu}	Emissivity of reciver insulating layer
$\eta_{shading}$	Shading factor
γ	Intercept factor
$\gamma_{stirling}$	Compression ratio of Stirling engine
λ_{ins}	Thermal conductivity of receiver insulating layer, W/(mK)
ρ	Reflectivity
θ_{dish}	Dish aperture angle (0° is horizental, 90° is vertically down)

Subscripts

i	Isentropic parameter
x	Stirling engine in column x
2	Water
2,1	Water at outlet of air-to-water heat exchanger and inlet of turbine
2,10	Water at outlet of evaporator and inlet of superheater
2,11	Water at outlet of superheater and inlet of air-to-water heat exchanger
2,2	Water at outlet of turbine and inlet of condenser
2,3	Water at outlet of turbine bleed point and inlet1 of deaerator
2,4	Water at outlet of condenser and inlet of condenser pump
2,5	Water at outlet of condenser pump and inlet of Stirling engine heat exchanger
2,6	Water at outlet of Stirling engine heat exchanger and inlet2 of deaeretor
2,7	Water at outlet of deaeretor and inlet of feed water pump
2,8	Water at outlet of feed water pump and inlet of preheater
2,9	Water at outlet of preheater and inlet of evaporator

References

[1] D.Y. Goswami. *Principles of Solar Engineering, Third Edition*. CRC Press, 2015.

[2] Giorgio Cau and Daniele Cocco. Comparison of medium-size concentrating solar power plants based on parabolic trough and linear Fresnel collectors. *Energy Procedia*, 45(0):101–110, 2014.

[3] G. Franchini, A. Perdichizzi, S. Ravelli, and G. Barigozzi. A comparative study between parabolic trough and solar tower technologies in Solar Rankine Cycle and Integrated Solar Combined Cycle plants. *Solar Energy*, 98(PC):302–314, 2013.

[4] Roberto Cipollone, Andrea Cinocca, and Angelo Gualtieri. A new conversion section for parabolic trough - Concentrated Solar Power (CSP-PT) plants. In *Energy Procedia*, volume 45, pages 61–70, 2014.

[5] Omar Behar, Abdallah Khellaf, Kamal Mohammedi, and Sabrina Ait-Kaci. A review of integrated solar combined cycle system (ISCCS) with a parabolic trough technology. *Renewable and Sustainable Energy Reviews*, 39(0):223–250, 2014.

[6] Sara Ghaem. Modeling and Analysis of Hybrid Solar-Dish Brayton Engine. *SolarPACES Conference*, 2012.

[7] F. Formosa and G. Despesse. Analytical model for Stirling cycle machine design. *Energy Conversion and Management*, 51(10):1855–1863, 2010.

[8] A.J. Juhasz. A mass computation model for lightweight brayton cycle regenerator heat exchangers. In *8th Annual International Energy Conversion Engineering Conference*, 2010.

[9] P.R. Fraser. *Stirling dish system performance prediction model*. Madison, 2008.

[10] Pablo Coronel and K. P. Sandeep. Heat transfer coefficient in helical heat exchangers under turbulent flow conditions. *International Journal of Food Engineering*, 4(1), 2008.

[11] R W Serth. *Process heat transfer principles and applications*. Elsevier Academic Press, Amsterdam; London, 2007.

[12] John A. Duffie and William A. Beckman. *Solar Engineering of Thermal Processes: Fourth Edition*. Wiley, 2013.

[13] R. E. Hogan. AEETES - a solar reflux receiver thermal performance numerical model. *Solar energy*, 52(2):167–178, 1994.

[14] Robert Y Ma. Wind effects on convective heat loss from a cavity receiver for a parabolic concentrating solar collector. *Sandia National Laboratory*, SAND92-7293(September), 1993.